Supporting Information

Heurich et al. 10.1073/pnas.1019338108

SI Materials and Methods

Genotyping. Consented (Cardiff University Ethics Committee; Internal Ref 07/18), healthy volunteers were screened for polymorphisms in the *CFH*, *CFB*, and *C3* genes by automated DNA sequencing of PCR amplified fragments. Genomic DNA was prepared from mucosal samples obtained by Catch-All Sample Collection swabs (Epicentre Biotechnologies) according to manufacturer's instructions. To confirm that the proteins used in our assays were identical except for the polymorphisms of interest, all exons and flanking regions from the *CFH*, *CFB*, and *C3* genes were amplified and sequenced in an ABI3730 sequencer using dye terminator cycle sequencing kit (Applied Biosystems) as previously described (1–3). Note that all $C3_{102R}$ donors were homozygote for $C3_{314P}$, and all $C3_{102G}$ donors were heterozygote $C3_{P314L}$. Linkage disequilibrium meant that among 1,300 individuals genotyped, it was not possible to identify a donor homozygote for both Gly102 and Pro314.

Purification of Native C3 from Plasma. C3 variant proteins were purified from plasma of $C3_{102}$ homozygote donors using classical chromatography. EDTA plasma was subjected to a 10% Na_2SO_4 cut and supernatant dialyzed into 10 mM potassium phosphate, pH 7.8, 5 mM benzamidine, 5 mM EDTA, and applied to a DEAE FF column (GE Healthcare). Protein was fractionated on a salt gradient to 0.4 M NaCl. C3-containing fractions were identified by SDS/PAGE, dialyzed into 50 mM Na-phosphate, pH 6, and applied to a Source S column (GE Healthcare). Protein was eluted on a gradient to 0.4 M NaCl; C3-containing fractions were pooled and dialyzed into Hepes-buffered saline, pH 7.4, for storage at −80 °C. C3 was further "polished" on day of assay as described by cation exchange (Mono S 5/5) and gel filtration (Superdex 200 10/300GL); all chromatography columns were from GE Healthcare. Hydrolyzed C3 [$C3(H_2O)$] was prepared by incubating C3 at 3 mg/mL with 50 mM hydroxylamine, pH 8.3, for 2 h at 25 °C. $C3(H_2O)$ was separated from residual C3 by ion exchange chromatography (Mono S 5/5), aggregates were removed by size exclusion chromatography (Superdex 200). Hydrolysis of the thioester was confirmed by inactivity of C3 (H_2O) in add-back hemolysis assays and by sensitivity of the alpha chain to fH/fI-mediated cleavage.

Generation of Recombinant fH (rfH1–4). DNA encoding the first 248 amino acid residues of fH (fH1–4) was purchased from Geneart and cloned into the pGMT7 expression plasmid (Invitrogen). Rosetta One Shot BL21 (DE3) *Escherichia coli* (Invitrogen) were transformed with plasmid by heat shock; colonies selected on ampicillin were expanded to OD_{600} of 0.5–0.6. Inclusion bodies were induced using 0.5 mM IPTG for 3 h. Bacteria were pelleted and lysed by sonication on ice in 10 mM Tris, pH 8, containing 10 mM $MgCl_2$, 150 mM NaCl, 10% glycerol. Inclusion bodies were harvested, incubated with 0.1 mg/mL DNase for 30 min, washed twice in Triton wash buffer (0.5% Triton 100, 50 mM Tris, 100 mM NaCl, 10 mM EDTA), resuspended in the same buffer without Triton, and solubilized in 6 M guanidine, 50 mM Tris, 100 mM NaCl, 2 mM EDTA. Proteins were refolded by rapid dilution 1:40 in 6 M urea/10 mM HCl and mixing at 4 °C with refold buffer (0.02 M ethanolamine, 1 mM EDTA, 0.5 M L-arginine, 1 mM cystamine dihydrochloride, 2 mM cysteamine hydrochloride, and 40 mL/mg protein). After 36 h, protein was dialyzed against 10 mM Tris, pH 8.1, and subjected to anion exchange chromatography on a Poros 50HQTM column (Applied Biosystems). Fractions containing rfH1–4 were pooled and passed over an anti-fH affinity column generated using a monoclonal antibody that recognizes a conformational epitope in native fH1–4 (IIB6, in-house). Eluted protein was gel filtered before Biacore analysis to remove aggregates and buffer exchange.

Generation of Depleted Sera for Hemolysis Assays. NHS was passed rapidly over respective affinity columns equilibrated in ice-cold buffer (10 mM Tris, pH 7.4, 150 mM NaCl). Columns (HiTrap 5 mL; GE Healthcare) were connected in series (anti-C3, MBI-C3-1; anti-fB, JC1; anti-fH, 35H9; all antibodies made in-house); fH was always depleted last in series to avoid spontaneous complement activation. C3 in depleted serum was below the detection limit (detection limit 0.043 mg/mL; normal range 0.75–1.65 mg/mL) when tested in a validated nephelometric assay (Clinical Biochemistry and Immunology Laboratory, University Hospital of Wales, Cardiff, United Kingdom); it exhibited minimal hemolytic activity compared with start material and was restored to >95% activity when reconstituted with pure C3. fB and fH levels in depleted sera were measured by ELISA. fB was below the assay detection limit (detection limit 4.5 μg/mL, normal range 54–245 μg/mL); fH was detected at 5 μg/mL (detection limit 0.1 μg/mL, normal range 124–402 μg/mL).

Alternative Pathway (AH_{50}) Assay. AH_{50} was measured essentially as described previously (4) with the following modification: C3 in serum was first inactivated by treatment with hydrazine (50 mM, pH 8.5, 2 h, 37 °C). Serum (R3) was dialyzed with multiple buffer changes against CFD before being passed over anti-fB and anti-fH affinity columns to generate NHS-R3ΔBH as described above. To generate serum containing specific variants, one volume each of C3 (1,000 μg/mL), fB (150 μg/mL), and fH (250 μg/mL) in AP buffer were mixed with one volume of NHS-R3ΔBH. Dilutions of this repleted serum (50 μL) were added to 50 μL rabbit E (2% vol/vol) and incubated at 37 °C for 30 min; lysis and AH_{50} were calculated as described (4).

fH Decay Hemolysis Assay. ShEA-C3b were generated using NHSΔC3BH with C3 add-back, and C3bBb was formed by incubating equal volumes of ShEA-C3b and 0.25 μg/mL fD mixed with 0.76 μM fB for 15 min at 37 °C. One volume of fH_{62V} (0.3–331 nM) in PBS/20 mM EDTA was added to the cells and incubated for 15 min at 37 °C. Lysis was developed by adding 1 volume NHS depleted of fH and fB (NHS△BH)(4% vol/vol) in PBS/20 mM EDTA and quantified as described above.

fH Cofactor Hemolysis Assay. ShEA-C3b were generated using NHSΔC3BH with C3 add-back, washed, and resuspended in AP buffer containing 4 μg/mL fI. An equal volume of fH (0.3–165 nM) was added and the mixture incubated at room temperature for 20 min. ShEA-C3b were washed and resuspended to 1 volume in AP buffer. To form convertase on residual C3b, an equal volume of AP buffer containing fB (44 nM) and fD (0.25 μg/mL) was added to the cells for 10 min at 37 °C. Lysis was developed as described above for the decay assay.

Surface Preparation for SPR (Biacore) and Data Analysis. For all kinetic analyses a CM5 chip (carboxymethylated dextran surface; GE Healthcare) was used; data were collected at 25 °C at a flow rate of 30 μL/min (proenzyme or convertase) or 20 μL/min (rfH1–4, sMCP, and sDAF). All kinetic data were double-referenced (data from reference cell and a blank inject subtracted). For fB and native fH kinetics, C3b variants (400 ± 20 RU) or $C3(H_20)$ (450 RU) were amine coupled according to the manufacturer's instructions (NHS/EDC coupling kit); the reference cell was ac-

tivated and blocked. For analysis of rfH1–4, sMCP, and sDAF binding affinities, 1,500 RU C3b was thioester coupled (rfH1–4 and sMCP) or amine coupled (sDAF) to the chip as described (5).

Kinetic parameters were analyzed using global fits; analysis used a "two-state conformational change" binding model for proenzyme and 1:1 Langmuir binding model for convertase formation (Biaevaluation T100 software, version 1.1). Affinity (K_D) of full-length factor H, rfH1–4, sMCP, and sDAF with immobilized C3b variants was analyzed using steady-state equilibrium analysis with the offset at zero.

1. Esparza-Gordillo J, et al. (2005) Predisposition to atypical hemolytic uremic syndrome involves the concurrence of different susceptibility alleles in the regulators of complement activation gene cluster in 1q32. *Hum Mol Genet* 14:703–712.
2. Pérez-Caballero D, et al. (2001) Clustering of missense mutations in the C-terminal region of factor H in atypical hemolytic uremic syndrome. *Am J Hum Genet* 68:478–484.
3. Martínez-Barricarte R, et al. (2010) Human C3 mutation reveals a mechanism of dense deposit disease pathogenesis and provides insights into complement activation and regulation. *J Clin Invest* 120:3702–3712.
4. Morgan BP (2000) *Complement Methods and Protocols*, ed Morgan BP (Humana Press, Clifton, New Jersey), pp 61–72.
5. Harris CL, Abbott RJ, Smith RA, Morgan BP, Lea SM (2005) Molecular dissection of interactions between components of the alternative pathway of complement and decay accelerating factor (CD55). *J Biol Chem* 280:2569–2578.

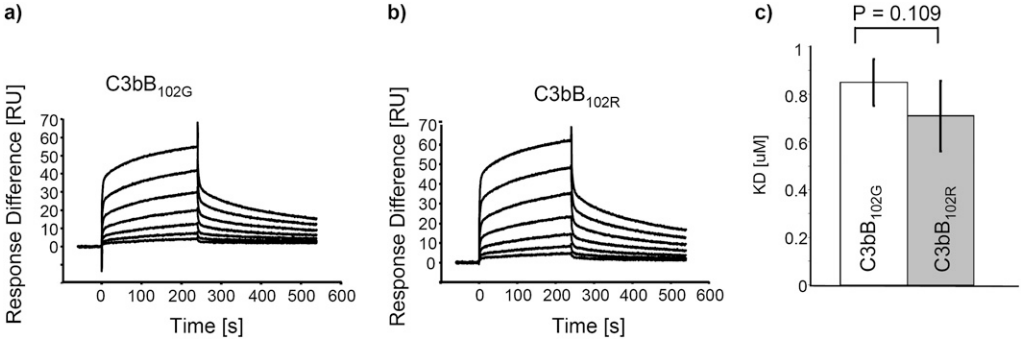

Fig. S1. Kinetics of proenzyme formation on $C3b_{R102G}$ variants. Native fB was flowed over either $C3b_{102G}$ (*A*) or $C3b_{102R}$ (*B*) at concentrations between 6 and 788 nM and binding response was measured. Affinity (K_D) was determined using a two-state reaction model. The affinity of fB for $C3b_{102G}$ (K_D = 0.85 ± 0.10 μM, n = 5) was not different from that for $C3b_{102R}$ (K_D= 0.71 ± 0.15 μM, n = 5). Multiple analyses on different days with different donors confirmed no significant difference in native fB (*C*) binding to the $C3b_{R102G}$ variants (two-tailed unpaired t test, P = 0.109).

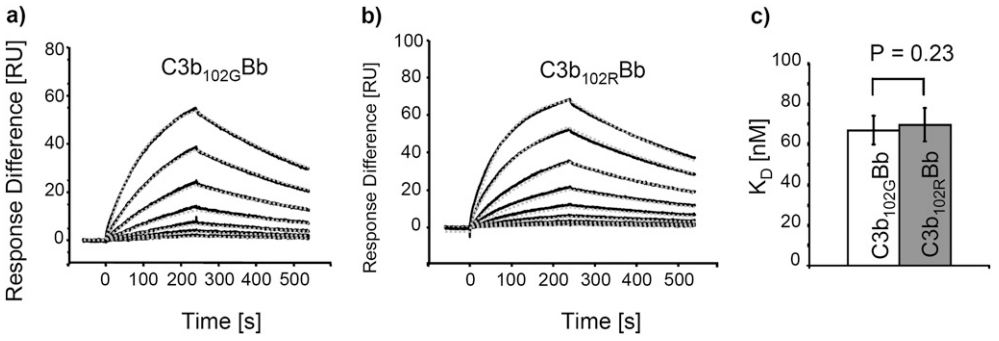

Fig. S2. Formation and decay of convertase formed by $C3b_{102G}$ or $C3b_{102R}$. C3b variants were amine coupled (400 ± 20 RU) to the chip surface and fB was flowed across the surface at concentrations between 3 nM and 397 nM in the presence of fD and Mg^{2+}. Sensorgrams illustrating convertase formation of $C3b_{102G}$ Bb (*A*) and $C3b_{102R}$ Bb (*B*) are solid black lines, fitted data are represented as gray dotted lines. (*C*) Kinetic analysis was performed multiple times, with global fitting being used for every experiment.

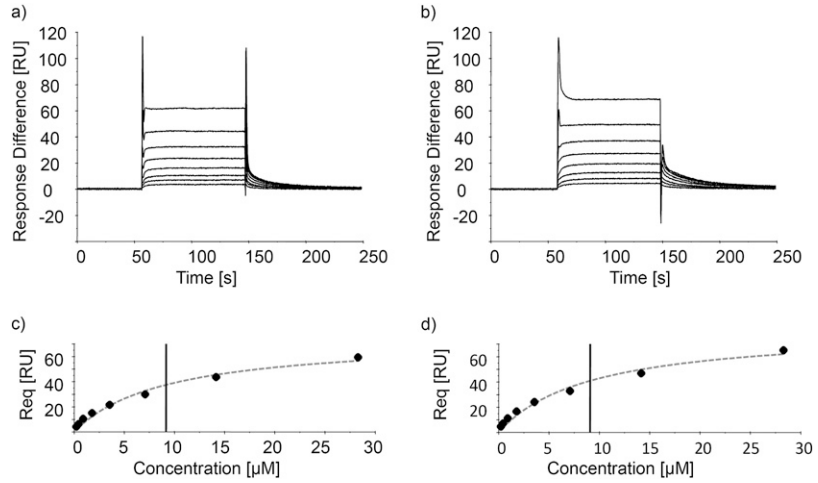

Fig. S3. Binding of native fH to $C3(H_20)_{R102G}$ variants. Native fH was flowed over immobilized $C3(H_20)_{102G}$ (*A*) or $C3(H_20)_{102R}$ (*B*) at concentrations between 0.2 μM and 28 μM and equilibrium binding response was measured. Affinity was determined by steady-state analysis for (*C*) $C3(H_20)_{102G}$, K_D = 9.02 ± 0.13 μM and (*D*) $C3(H_20)_{102R}$, K_D = 8.85 ± 0.64 μM).

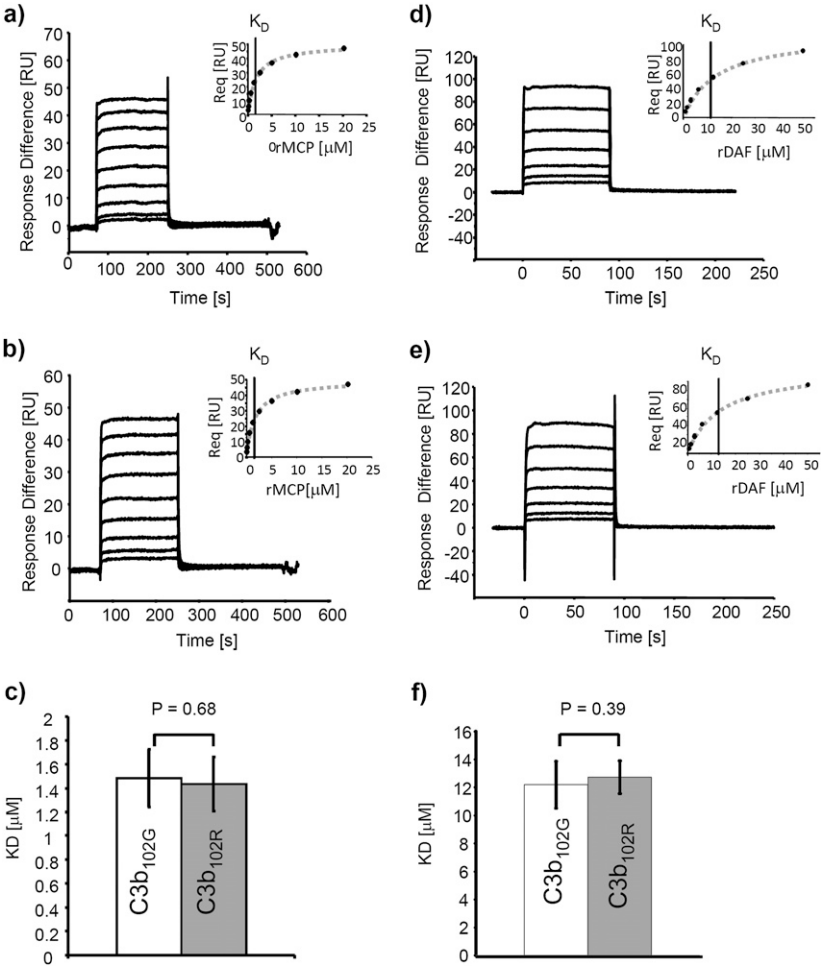

Fig. S4. Binding of sMCP and sDAF to $C3b_{R102G}$ variants. Recombinant sMCP (100 nM–20 μM) and sDAF (0.78–50 μM) were flowed over either $C3b_{102G}$ (*A* and *D*) or $C3b_{102R}$ (*B* and *E*) and binding response was measured. Affinity (K_D) was determined at steady state. The affinity of sMCP for $C3b_{102G}$ (K_D = 1.48 ± 0.23 μM, n = 11) was not different from that for $C3b_{102R}$ (K_D = 1.43 ± 0.22 μM, n = 6); sDAF affinity for $C3b_{102G}$ (K_D = 12.21 ± 1.69 μM, n = 19) was not different from that for $C3b_{102R}$ (K_D = 12.75 ± 1.18 μM, n = 10). Multiple analyses of $C3b_{R102G}$ binding on different days and with different donors (*C* and *F*) confirmed that there was no significant difference for sMCP (P = 0.68) or sDAF (P = 0.39) (two-tailed unpaired t test).

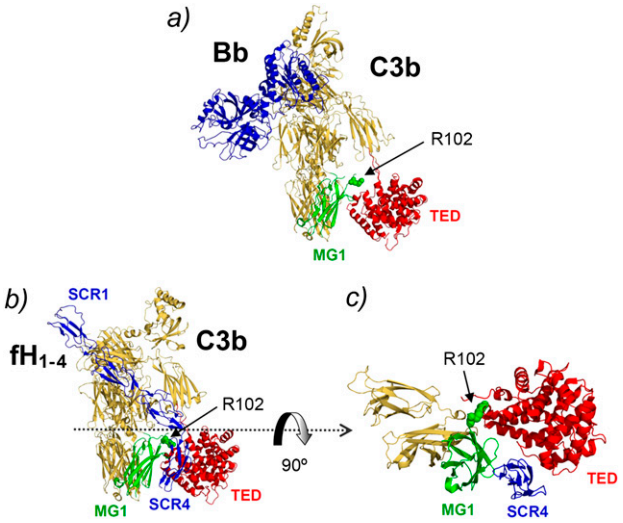

Fig. S5. Modeling the $C3b_{R102G}$ polymorphism. (*A*) Model of the AP C3 convertase (C3bBb) based on the atomic structure of the AP C3 convertase stabilized with the bacterial inhibitor SCIN (PDB ID 2WIN) (1). Color codes: C3b is shown in light orange, Bb in blue. MG1 and TED domains of C3b are highlighted in green and red, respectively. The R102 residue in MG1 is shown in solid spheres. Note that residue R102 is located distant from the site of interaction between C3b and Bb. (*B*) Atomic structure of C3b in complex with fH1–4 (PDB ID 2W11) (2). Color codes: fH is shown in blue with the positions of SCR1 (N terminal) and SCR4 (C terminus) indicated, C3b is shown in light orange. MG1 and TED domains of C3b are highlighted in green and red, respectively. (*C*) To better illustrate the potential consequences of the R102G substitution in the C3b-fH1–4 complex, the top part of the complex in the model (above the discontinuous line) is removed and the remaining structure tilted 90° (color codes as in *B*). Note that R102 is located in a positively charged area at the interface between the MG1 domain and a negatively charged area on TED and likely contributes to stabilizing the MG1-fH(SCR4)-TED complex. Substitution of neutral Gly at position 102 should reduce the negative charge in the MG1 domain, likely decreasing the strength of the MG1-TED interaction, which in turn weakens the fH-C3b interaction.

1. Rooijakkers SH, et al. (2009) Structural and functional implications of the alternative complement pathway C3 convertase stabilized by a staphylococcal inhibitor. *Nat Immunol* 10: 721–727.
2. Wu J, et al. (2009) Structure of complement fragment C3b-factor H and implications for host protection by complement regulators. *Nat Immunol* 10:728–733.